Results in Chemistry 6 (2023) 101099

Contents lists available at ScienceDirect

Results in Chemistry

journal homepage: www.sciencedirect.com/journal/results-in-chemistry

New metal complexes containing a methyldopa Schiff base for carbon dioxide storage

Noor Emad [a], Gamal A. El-Hiti [b,*], Emad Yousif [a], Dina S. Ahmed [c], Marwa Fadhil [a], Benson M. Kariuki [d]

[a] Department of Chemistry, College of Science, Al-Nahrain University, Baghdad 64021, Iraq
[b] Department of Optometry, College of Applied Medical Sciences, King Saud University, Riyadh 11433, Saudi Arabia
[c] Department of Chemical Industries, Institute of Technology-Baghdad, Middle Technical University, Baghdad, Iraq
[d] School of Chemistry, Cardiff University, Main Building, Park Place, Cardiff CF10 3AT, UK

ARTICLE INFO

Keywords:
Methyldopa Schiff base
Metal complexes
Carbon dioxide storage media
Mesoporous
Surface area

ABSTRACT

The high concentration of carbon dioxide in the environment, including from the burning of fossil fuels to meet our energy requirements, is a pressing environmental concern that requires urgent attention. As a result, the development of novel materials for storing gases such as carbon dioxide and hydrogen has garnered greater attention in research. The current work reports the synthesis of a Schiff base derived from methyldopa and its metal complexes. In addition, their effectiveness as carbon dioxide storage materials were assessed. The reaction of methyldopa and 4-hydroxybenzaldehyde in boiling ethanol under acidic conditions for four hours gave the corresponding Schiff base in excellent yield. The reaction of metal (copper, cobalt, and nickel) chlorides and Schiff base in boiling ethanol for three hours gave the corresponding metal complexes in high yields (77–83%). The surface morphology and surface area of the synthesized metal complexes were evaluated. The mesoporous complexes have a surface area that ranges from 3.59 to 7.36 m^2/g. The average pores diameter was 7.75–12.27 nm, and the pores volume was 0.0.11–0.014 cm^3/g. The carbon dioxide storage capacity of the synthesized mesoporous complexes was 27.4–30.6 cm^3/gm. The complex containing nickel was the most efficient towards carbon dioxide uptake (30.6 cm^3/cm) possibility due to its relatively high surface area (7.36 cm^2/g) and pores volume (0.014 cm^3/g) compared to the copper and cobalt complexes.

Introduction

One of the most common natural greenhouse gases is carbon dioxide (CO_2) [1]. The gas traps heat within the atmosphere, resulting in global warming. The global rise in temperature has increased substantially since the middle of the last century [2,3]. Global warming continues to escalate alarmingly [4,5]. The increase in global temperature has resulted in significant environmental threats, such as the melting of Arctic ice, with the potential to cause, for example, floods and droughts [6]. Another effect of the rise in atmospheric CO_2 concentration is the increased acidity of the oceans. The main reason for the rise in CO_2 emissions into the atmosphere is the increased consumption of fossil fuels driven by human activities [7–9].

The challenge is to moderate CO_2 levels in the atmosphere. This can be achieved through different approaches. One effective strategy is to use renewable and green energy (e.g., nuclear power, biomass, wind power, and solar energy) instead of relying solely on fossil fuels [10]. The use of these forms of energy is appealing because of the associated decrease in CO_2 emissions [11]. Unfortunately, these energy sources are currently insufficient to meet the global demand, and competition with the prices of fossil fuels is not in their favor [12]. Another approach to limiting the levels of CO_2 in the atmosphere is to capture the gas and store it in materials that serve as storage media [13].

The sorption of CO_2 can be controlled by varying conditions, such as pressure and temperature, and can occur either physically or chemically [14–18]. Typically, the capture of CO_2 requires its separation and adsorption at high pressure using absorbent materials [19–22]. A lot of current research is dedicated to developing materials that can capture CO_2 selectively [23–25]. Numerous adsorbent materials have been synthesized and utilized for CO_2 storage. For practical application, these materials should be economical to produce, reusable, chemically stable, and not harmful to humans and the environment. Fundamentally, the

* Corresponding author.
E-mail address: gelhiti@ksu.edu.sa (G.A. El-Hiti).

https://doi.org/10.1016/j.rechem.2023.101099
Received 22 August 2023; Accepted 4 September 2023
Available online 9 September 2023

materials must possess a relatively large accessible surface area, usually associated with a rough surface, and appropriate pores size and volume [26]. Activated carbon, ionic liquids, amines, silica, metal oxides, zeolites, metal–organic frameworks, cross-linked polymers, and porous organic polymers are the most commonly used CO_2 adsorbents [27–31]. However, these adsorbents have various disadvantages. For example, the use of amines is hindered by their toxicity and volatility [32]. Metal oxides have a low capacity to capture CO_2 [33,34], and activated carbons have poor selectivity [35–39]. Even though organic polymers can have high surface areas [40–42], the synthetic methods are not green [43,44]. Thus, further improvements are needed, and recently, some progress has been made in the use of metal complexes as storage media for CO_2 [45–48].

Schiff bases are rich in heteroatoms (e.g., nitrogen and oxygen) and have been tested as storage media for CO_2 [49]. In addition, metal complexes can capture CO_2 [45–48]. Therefore, the exploration of metal complexes containing Schiff bases as CO_2 storage media is appealing. Methyldopa is an antibiotic containing aromatic rings and heteroatoms (nitrogen and oxygen) [50]. Its Schiff base was selected as the organic moiety in organometallic complexes. Here, we now report the successful capture of CO_2 over new metal complexes of a methyldopa Schiff base.

Experimental section

Materials and methods

Methyldopa (99.5%), other chemicals, reagents, and solvents were obtained from different suppliers and were used as received. Melting points were determined using the hot-stage Gallenkamp melting point apparatus. The microanalyses were performed on Shimadzu's AA-680 atomic absorption spectrometer. The FTIR spectra were obtained on Bruker Alpha spectrometer. The UV spectra were recorded at 25 °C in dimethyl sulfoxide on a Shimadzu UV-1601 UV–VIS spectrophotometer using a 1.0 cm quartz cell. The ^{1}H (400 MHz) and ^{13}C NMR (100 MHz) spectra were acquired on a Bruker AV400 spectrometer. Isotherms were evaluated using the MicroActive TriStar II Plus (Version 2.03). The specific surface area was measured using the Brunauer-Emmett-Teller (BET) method. The pores size distribution (pore sizes, diameter, and size) was identified using the Barrett-Joyner-Halland (BJH) theory. A TESCAN MIRA3 LMU system at an accelerating voltage of 15 kV was used to capture the scanning electron microscopy (FESEM) images. A Veeco instrument was used to record the images of atomic force microscopy (AFM). The complexes were dried in a vacuum oven (70 °C, 6 h) under a nitrogen flow. The pore volumes were determined at a relative pressure (P/P°) 0.98. The CO_2 uptake was carried out on an H-sorb 2600 high-pressure volumetric adsorption analyzer (40 bars, 323 K).

Synthesis of (S,E)-3-(3,4-dihydroxyphenyl)-2-((4-hydroxybenzylidene) amino)-2-methylpropanoic acid

A mixture of methyldopa (4.22 g, 20 mmol) and 4-hydroxy benzaldehyde (2.44 g, 20 mmol) in EtOH (20 mL) containing HOAc (0.1 mL) was refluxed for 4 h. The mixture was cooled to room temperature, and the solid formed was collected by filtration, washed with EtOH, and dried to give the corresponding Shiff base as a white solid (85%), Mp 232–234 °C. FTIR (cm^{-1}) 3154, 1666, 1589, 1449. ^{1}H NMR (DMSO-d_6) 9.76 (s, 1H, OH), 8.07 (s, 1H, CH), 7.75 (d, J = 8.5 Hz, 2H, Ar), 6.97 (d, J = 8.5 Hz, 2H, Ar), 6.72 (s, 2H, 2 OH), 6.83 (d, J = 8.0 Hz, 1H, Ar), 6.54 (dd, J = 8.0 and 2.0 Hz, 1H, Ar), 6.02 (s, 1H, Ar), 2.93 (d, J = 12 Hz, 1H), 2.72 (d, J = 12 Hz, 1H), 1.45 (s, 3H, Me). ^{13}C NMR (DMSO-d_6) 35.2, 42.8, 61.0, 115.8, 116.6, 118.6, 121.7, 124.0, 126.6, 128.4, 132.5, 145.0, 145.5, 164.8, 173.9. Anal. Calcd. for $C_{17}H_{17}NO_5$ (315.33): C, 64.75; H, 5.43; N, 4.44. Found: C, 64.76; H, 5.45; N, 4.45%.

Synthesis of metal complexes

A stirred mixture of Schiff base (3.15 g, 10 mmol) and appropriate metal chloride ($CoCl_2$, $NiCl_2{\cdot}6H_2O$, and $CuCl_2{\cdot}2H_2O$; 5 mmol) in EtOH (20 mL) was refluxed for 3 h. The solid formed was filtered, washed with boiling EtOH, and dried to give the corresponding metal complex in good yield (Table 1).

Result and discussion

Synthesis of metal complexes

The reaction of equimolar quantities of methyldopa and 4-hydroxybenzaldehyde in boiling EtOH in the presence of glacial acetic acid (AcOH) as a catalyst for 4 h gave the corresponding Schiff base in 85% yield Scheme 1).

The FTIR spectrum of the Schiff base showed strong absorption bands at 1666 and 1589 cm^{-1} due to the C = O and the CH = N groups, respectively [51,52]. ^{1}H NMR spectrum of the Schiff base showed a singlet at 8.07 ppm due to the CH = N proton. Furthermore, it revealed the presence of two sets of doublets, each consisting of one proton, at 2.93 and 2.72 ppm. These doublets can be attributed to the CH_2 protons. There was no signal detected for the carboxyl proton. The ^{13}C NMR spectrum displayed a signal downfield at 173.9 ppm, which was attributed to the carbon of the carbonyl group. At the same time, the CH = N carbon appeared at 164.8 ppm. In addition, it showed three signals at a high field at 35.2, 42.8, and 61.0 ppm due to the methyl, methylene, and the N–C carbons, respectively.

The reaction of Schiff base and metal chlorides ($CoCl_2$, $NiCl_2{\cdot}6H_2O$, and $CuCl_2{\cdot}2H_2O$) in boiling EtOH for 3 h gave the corresponding metal complexes (Scheme 2) in high yields (Table 1). The reaction involves using excess (two-mole equivalents) Schiff base without a catalyst.

The FTIR spectra of metal complexes showed absorption bands at 3126–3177 cm^{-1} due to the vibration of the OH group (Table 2). The CH = N absorption band appeared within the region of 1585–1588 cm^{-1}. In addition, the M−O absorption band appeared in the 421–508 cm^{-1} region. The asymmetric (asym) and symmetric (sym) vibration bands for the carboxylate group appeared at 1650–1663 and 1446–1449 cm^{-1} regions, respectively. The difference (Δv) between the carboxylate group's asym and sym vibration frequencies ranged from 201 to 214 cm^{-1}. The calculated Δv shows an anisobidentate asymmetry, a state between monodentate and bidentate [53,54].

The UV spectral data, magnetic susceptibility ($\mu_{eff.}$), geometry, and hybridization type of the metal complexes are summarized in Table 3. The UV spectrum of the Ni complex showed four absorption bands at 414,938, 30,581, 23,809, and 21,008 cm^{-1} due to the $\pi \rightarrow \pi^*$, $n \rightarrow \pi^*$, $^3A_2g(F) \rightarrow {}^3T_1g(P)$, and $^3A_2g(F) \rightarrow {}^3T_1g(F)$, respectively. In contrast, the Cu and Co complexes showed six and five absorption bands, respectively. The Co and Ni complexes have an octahedral geometry with an μ_{eff} 4.5 and 3.2 BM, respectively [55]. In contrast, the Cu complex has a distorted octahedral geometry with an μ_{eff} of 1.7 BM [55]. The Co and Ni complexes had a sp^3d^2 high spin hybridization [56]. On the other hand, the Cu complex has a sp^3d^2 hybridization. The molar conductivity of the metal complexes was 0 μS/cm, indicating a non-electrolyte state [46].

Surface morphology of metal complexes

The surface morphology of the metal complexes was examined using FESEM [57]. The undistorted FESEM images indicated that the surfaces of the synthesized metal complexes were uneven and had pores that varied in shape and size (Fig. 1). The particle sizes for the Cu, Co, and Ni complexes were 22.3–53.6 nm, 37.2–164.8 nm, and 17.9–51.4 nm, respectively.

The AFM offers accurate details on the level of porosity and roughness present on the surfaces of materials [58]. In addition, it provides information that enables a complete understanding of the lattice

Table 1
Physical properties of metal complexes.

Complex	Color	Mp (°C)	Yield (%)	Elemental analysis: calculated (found; %)			
				C	H	N	M
Cu	Brown	110–112	81	59.00 (59.03)	4.66 (4.68)	4.05 (4.10)	9.18 (9.21)
Co	Brown	116–118	83	59.39 (59.41)	4.69 (4.71)	4.07 (4.11)	8.57 (8.62)
Ni	Green	95–97	77	59.41 (59.44)	4.69 (4.73)	4.08 (4.14)	8.54 (8.55)

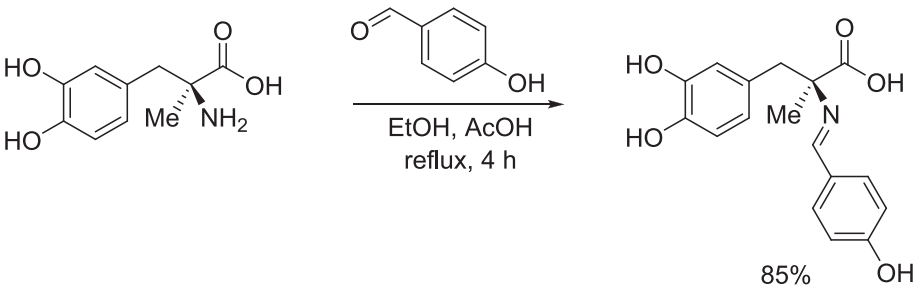

Scheme 1. Synthesis of methyldopa Schiff base.

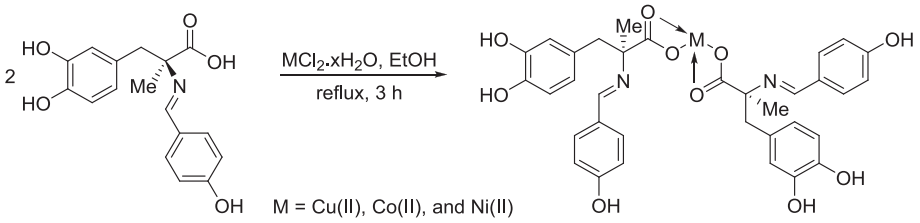

Scheme 2. Synthesis of metal complexes.

Table 2
Selected FTIR absorption bands of metal complexes.

Complex	OH	CH = N	C = O			M–O
			asym	sym	Δv (asym - sym)	
Cu	3177	1585	1654	1446	208	438
Co	3126	1588	1663	1449	214	421
Ni	3138	1586	1650	1449	201	508

structure of various minerals and evaluates the three-dimensional geometric characteristics of individual particles. The AFM images of the synthesized complexes indicated uneven surfaces and mesoporous structures (Fig. 2). The roughness factor for the Cu, Co, and Ni complexes was determined to be 250.3 nm, 265.2 nm, and 274.1 nm, respectively. Rough surfaces are advantageous for gas adsorption, so the metal complexes were anticipated to be effective in capturing CO_2.

Nitrogen gas adsorption and pore size determination of complexes

The surfaces of the metal complexes were subjected to nitrogen gas adsorption at 77 K and 40 bar (Figs. 3–5). The specific surface areas of metal complexes were evaluated by the BET method [59]. The isotherms were Type III with no monolayers and showed relatively weak interactions between CO_2 and metal complexes [61]. A similar adsorption and condensation heat was observed. The CO_2 uptake increased as the pressure increased. Table 4 summarizes the size and diameter of pores

Table 3
UV spectral data of metal complexes.

Complex	λ (nm)	Band (cm^{-1})	Transition	μ_{eff}, (BM)	Geometry	Hybridization
Cu	206	48,544	π → π*	1.7	Distorted octahedral	sp^3d^2
	242	41,322				
	271	36,900				
	336	29,762	n → π*			
	457	21,882	LMCT			
	552	18,116	$^2Eg \rightarrow {}^2T_2g$			
Co	205	48,780	π → π*	4.5	Octahedral	sp^3d^2 high spin
	272	36,765				
	340	29,412	n → π*			
	500	20,000	$^4T_1g(F) \rightarrow {}^4T_1g(P)$			
	600	16,667	$^4T_1g(F) \rightarrow {}^4T_1g(P)$			
Ni	241	414,938	π → π*	3.2	Octahedral	sp^3d^2 high spin
	327	30,581	n → π*			
	420	23,809	$^3A_2g(F) \rightarrow {}^3T_1g(P)$			
	476	21,008	$^3A_2g(F) \rightarrow {}^3T_1g(F)$			

LMCT = ligand-to-metal charge transfer.

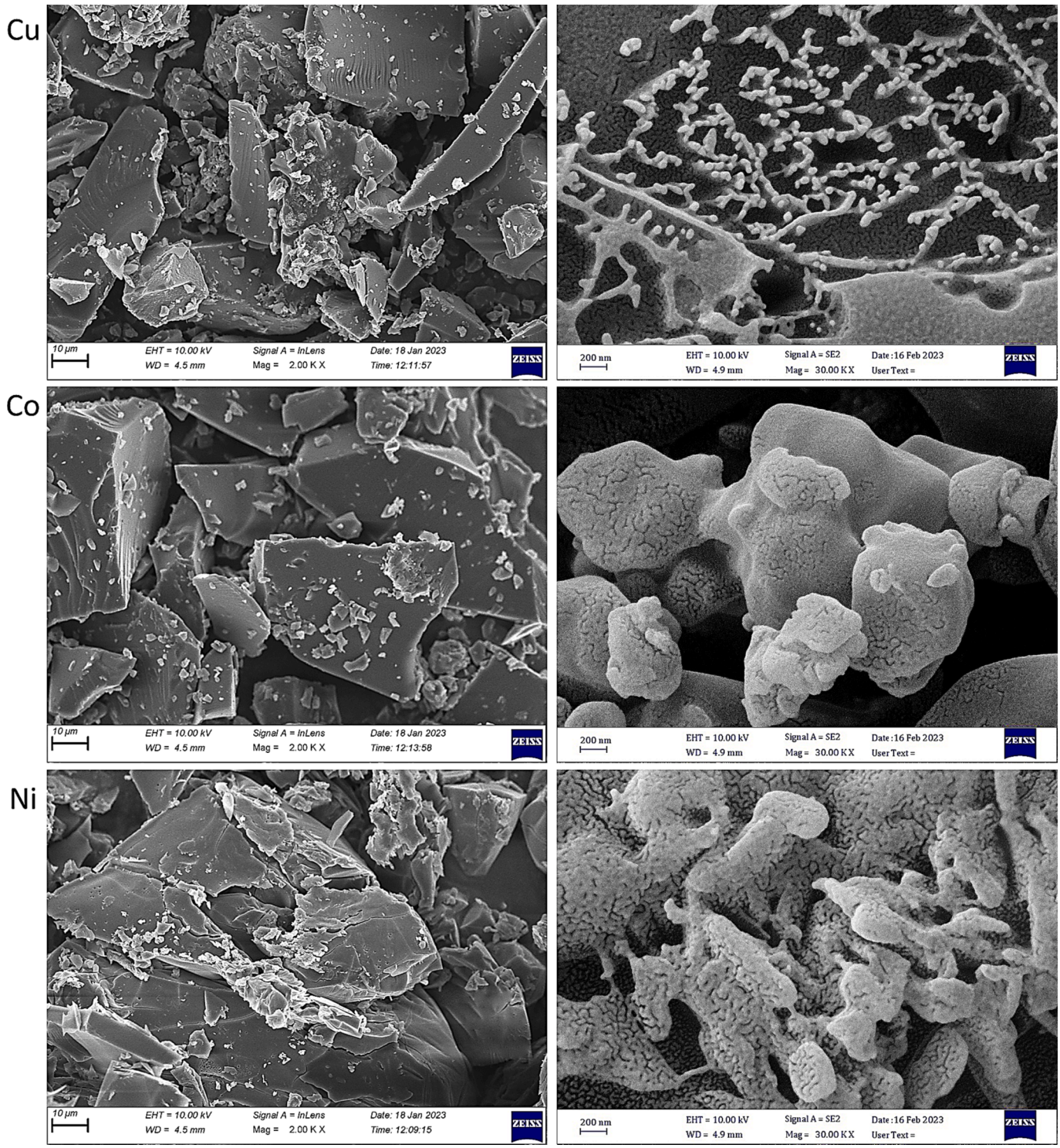

Fig. 1. FESEM images of metal complexes.

and the specific surface of metal complexes.

The specific surface area and pore volume reflect the structures of metal complexes and are associated with their adsorption capacity [60]. The specific surface area is determined by the size of the pores and not their volume. Gas adsorption typically relies on factors such as the specific surface area, volume of pores, and the distribution of their sizes. The mesoporous structures of metal complexes had an average pore diameter varying from 7.75 to 11.99 nm. The Ni complex has the smallest pore diameter of 7.75 nm but boasts the largest specific surface area of 7.36 m^2/g and pore volume of 0.014 cm^3/g.

Carbon dioxide storage of complexes

The temperature, pressure, pores volume, and surface area of adsorbents are the main factors affecting the uptake of CO_2. The level of interaction between polarized bonds of absorbents and CO_2 is also essential [62]. The pressure was varied from 1 to 40 bar. The highest CO_2 adsorption was obtained when the pressure was set at 40 bar and the temperature at 323 K (Fig. 6). The metal complexes have a similar ability to capture CO_2. The Ni complex led to the highest CO_2 uptake (30.6 cm^3/g) compared to the other two. The Ni complex has the largest

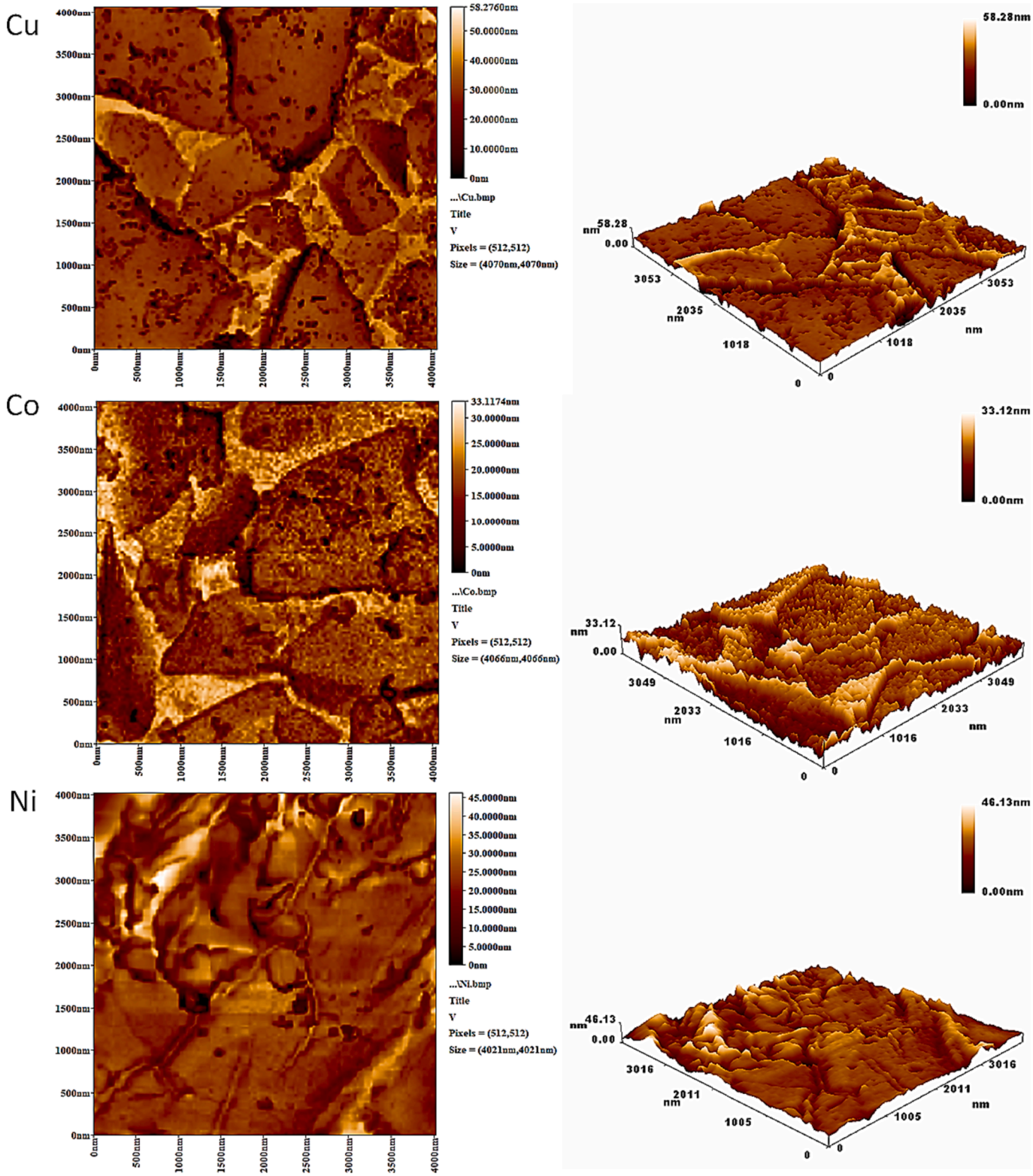

Fig. 2. AFM images for metal complexes.

surface area and pore volume.

Table 5 shows the CO_2 uptake (323 K, 40–50 bar) and surface area of various metal complexes containing different organic moieties. Despite the small surface area, the synthesized metal complexes showed a higher ability to adsorb CO_2 than those with carvedilol. [45]. Furthermore, they demonstrated a similar ability to adsorb CO_2 as metal complexes containing different organic components. CO_2 is postulated to be adsorbed onto metal complexes through physisorption, where the interaction between the heteroatoms of the adsorbents and the oxygen of CO_2 controls the adsorption process [14].

Conclusions

A convenient procedure was utilized to synthesize three mesoporous

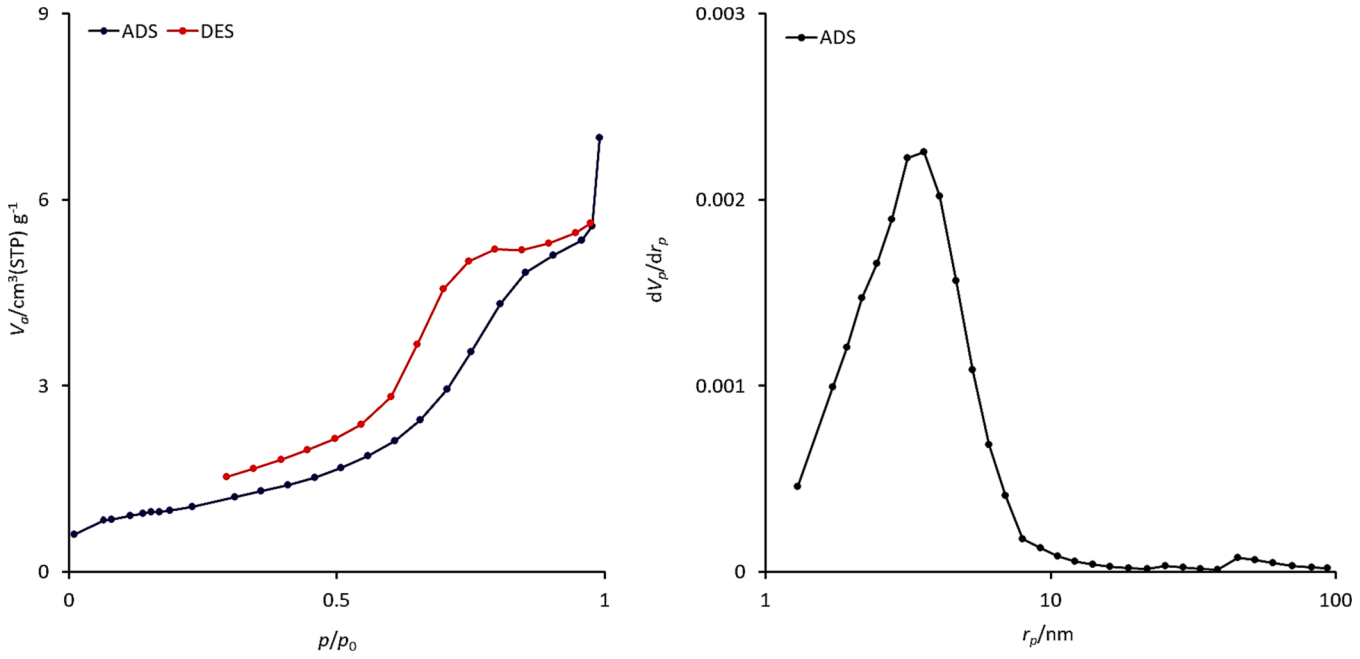

Fig. 3. The (a) N_2 adsorption (ADS) and desorption (DES) isotherms and (b) pore size distribution of Cu complex.

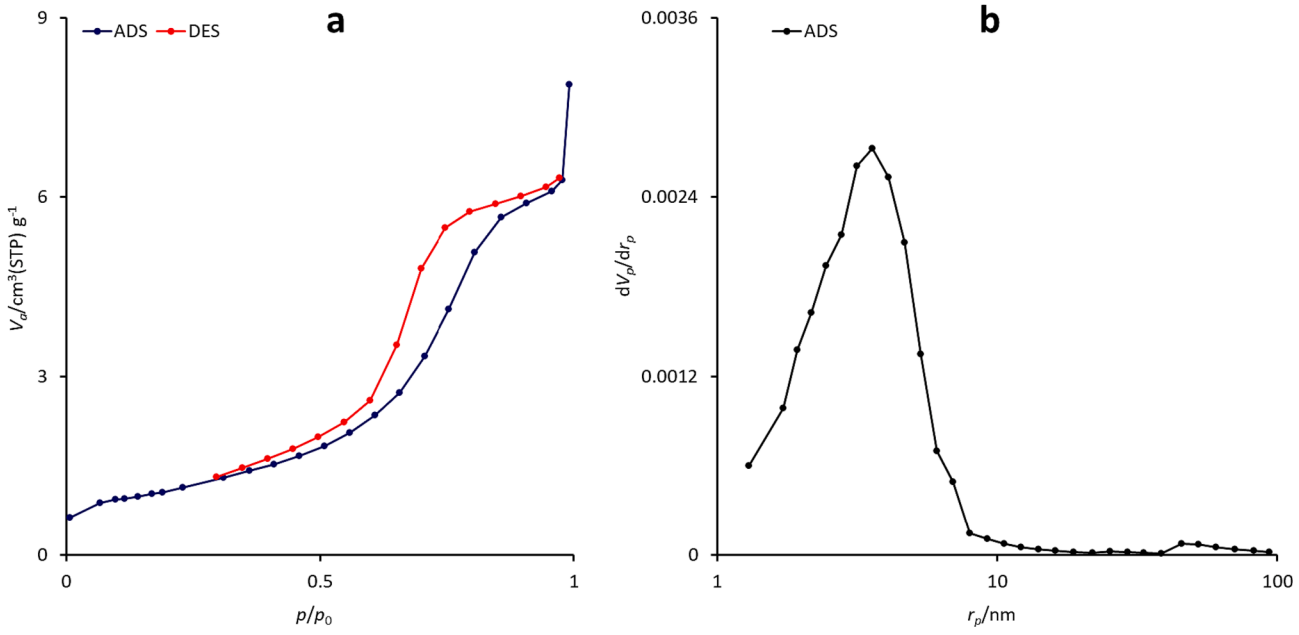

Fig. 4. The (a) N_2 adsorption (ADS) and desorption (DES) isotherms and (b) pore size distribution of Co complex.

metal complexes in high yields. The surface of metal complexes is rough, a property that promotes the effective adsorption of carbon dioxide. The metal complexes have a relatively narrow range of surface area (3.59–7.36 m^2/g), average pores diameter (7.75–12.27 nm), and pores volume (0.0.11–0.014 cm^3/g). The complexes absorbed carbon dioxide, and their capacity was similar (27.4–30.6 cm^3/gm). The nickel complex has the highest surface area at 7.36 cm^2/g and the largest pores volume at 0.014 cm^3/g, leading to the highest carbon dioxide uptake (30.6 cm^3/cm).

CRediT authorship contribution statement

Noor Emad: Investigation, Writing – review & editing, Writing – original draft. **Gamal A. El-Hiti:** Conceptualization, Methodology, Writing – review & editing, Funding acquisition, Software, Formal analysis, Writing – original draft, Data curation, Resources. **Emad Yousif:** Conceptualization, Methodology, Validation, Writing – review & editing, Software, Formal analysis, Writing – original draft, Data curation, Supervision. **Dina S. Ahmed:** Methodology, Validation, Writing – review & editing, Software, Formal analysis, Writing – original draft, Data curation. **Marwa Fadhil:** Investigation, Writing – review & editing, Writing – original draft. **Benson M. Kariuki:** Validation, Writing – review & editing, Software, Formal analysis, Writing – original draft.

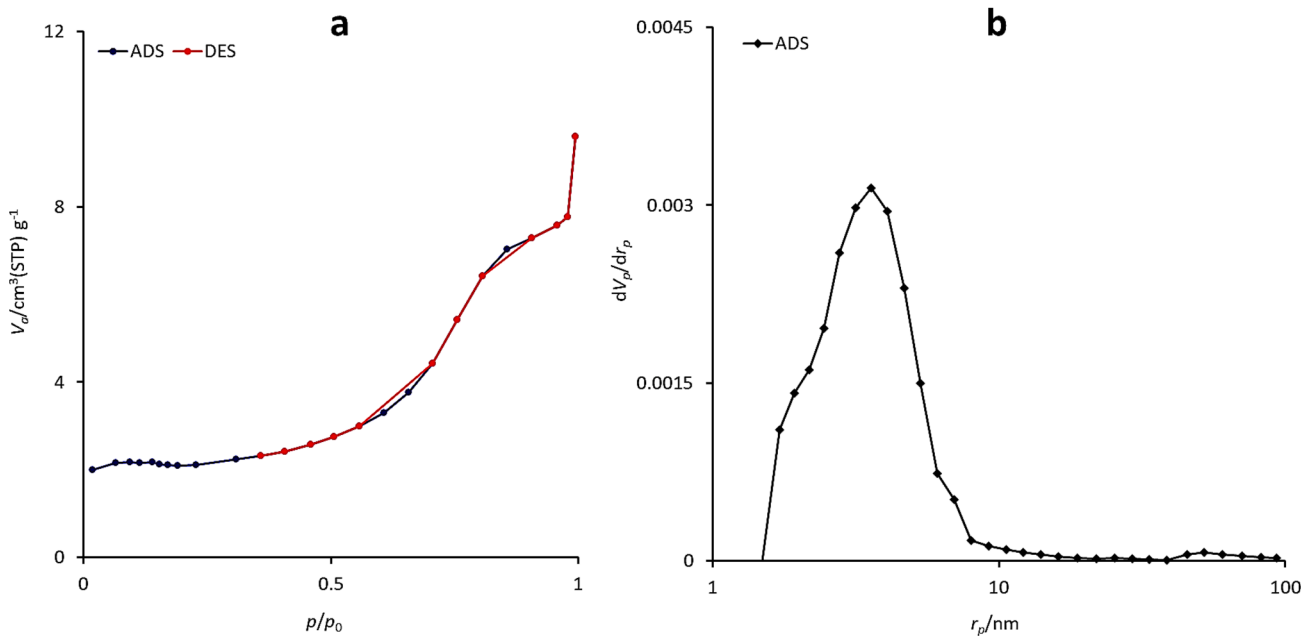

Fig. 5. The (a) N_2 adsorption (ADS) and desorption (DES) isotherms and (b) pore size distribution of Ni complex.

Table 4
Surface areas, pore volume, and diameter of metal complexes.

Complex	S_{BET} (m^2/g)	Pore volume (cm^3/g)	Average pore diameter (nm)
Cu	3.59	0.011	11.99
Co	3.91	0.012	12.27
Ni	7.36	0.014	7.75

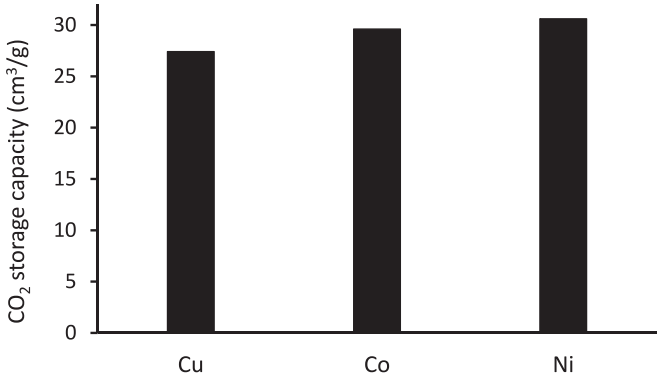

Fig. 6. The CO_2 storage capacity of metal complexes.

Table 5
CO_2 uptake (323 K, 40–50 bar) and surface area of metal complexes containing different organic moieties.

Organic unit in metal complexes	S_{BET} (m^2/g)	CO_2 (cm^3/g)	Reference
Methyldopa	3.6–7.4	27.4–30.6	Current research
Carvedilol	6.1–9.1	10.5–18.2	45
Valsartan	16.0–22.8	24.1–34.5	46
Fusidate	31.2–46.9	32.2–34.8	47
Telmisartan	32.4–130.4	16.5–35.0	48

Declaration of Competing Interest

The authors declare that they have no known competing financial interests or personal relationships that could have appeared to influence the work reported in this paper.

Data availability

Data will be made available on request.

Acknowledgments

We thank Al-Nahrain University for its technical support. G. A. El-Hiti acknowledges the support received from the Researchers Supporting Project (number RSP2023R404), King Saud University, Riyadh, Saudi Arabia.

References

[1] M. Zubair, S. Chen, Y. Ma, X. Hu, Sustainability 15 (2023) 4817, https://doi.org/10.3390/su15064817.
[2] A.A. Olajire, L. Azeez, E.A. Oluyemi, Chemosphere 84 (2011) 1044–1051, https://doi.org/10.1016/j.chemosphere.2011.04.074.
[3] R. Uning, M.T. Latif, M. Othman, L. Juneng, N.M. Hanif, M.S.M. Nadzir, K.N. A. Maulud, W.S.W.M. Jaafar, N.F.S. Said, F. Ahamad, M.S. Takriff, Sustainability 12 (2020) 5077, https://doi.org/10.3390/su12125077.
[4] S. Sun, H. Sun, P.T. Williams, C. Wu, Sustain, Energy Fuels 5 (2021) 4546–4559, https://doi.org/10.1039/D1SE00797A.
[5] L. Wang, L. Wang, Y. Li, J. Wang, Decis, The Analysts Journal 7 (2023), 100237, https://doi.org/10.1016/j.dajour.2023.100237.
[6] K. Abbass, M.Z. Qasim, H. Song, M. Murshed, H. Mahmood, I. Younis, Environ. Sci. Pollut. Res. 29 (2022) 42539–42559, https://doi.org/10.1007/s11356-022-19718-6.
[7] A. Mardani, D. Streimikiene, F. Cavallaro, N. Loganathan, M. Khoshnoudi, The Science of the Total Environment 649 (2019) 31–49, https://doi.org/10.1016/j.scitotenv.2018.08.229.
[8] H. Sun, Q. Xin, Z. Ma, S. Lan, Environmental Science and Pollution Research 26 (2019) 5076–5082, https://doi.org/10.1007/s11356-018-3988-5.
[9] Z. Liu, Z. Deng, S.J. Davis, C. Giron, P. Ciais, Nat. Rev. Earth Environ. 3 (2022) 217–219, https://doi.org/10.1038/s43017-022-00285-w.
[10] A. Qazi, F. Hussain, N.A. Rahim, G. Hardaker, D. Alghazzawi, K. Shaban, K. Haruna, IEEE Access 7 (2019) 63837, https://doi.org/10.1109/ACCESS.2019.2906402.
[11] N.A. Ludin, N.I. Mustafa, M.M. Hanafiah, M.A. Ibrahim, M.A.M. Teridi, S. Sepeai, A. Zaharim, K. Sopian, Renew. Sust. Energy. Rev. 96 (2018) 11–28, https://doi.org/10.1016/j.rser.2018.07.048.
[12] Y. Ouyang, H. Yang, P. Zhang, Y. Wang, S. Kaur, X. Zhu, Z. Wang, Y. Sun, W. Hong, Y.F. Ngeow, H. Wang, Molecules 22 (2017) 1592, https://doi.org/10.3390/molecules22101592.
[13] A.I. Osman, M. Hefny, M.I.A.A. Maksoud, A.M. Elgarahy, D.W. Rooney, Environ. Chem. Lett. 19 (2021) 797–849, https://doi.org/10.1007/s10311-020-01133-3.

[14] A.A. Abd, S.Z. Naji, A.S. Hashim, M.R. Othman, J. Environ. Chem. Eng. 8 (2020), 104142, https://doi.org/10.1016/j.jece.2020.104142.
[15] O.H.P. Gunawardene, C.A. Gunathilake, K. Vikrant, S.M. Amaraweera, Atmos. 13 (2022) 397, https://doi.org/10.3390/atmos13030397.
[16] H. Zeng, X. Qu, D. Xu, Y. Luo, Front. Chem. 10 (2022), 939701, https://doi.org/10.3389/fchem.2022.939701.
[17] D. Krishnaiah, A. Bono, S.M. Anisuzzaman, C. Joseph, T.B. KheeJ. Appl. Sci. 14 (2014) No.: 3142–3148. 10.3923/jas.2014.3142.3148.
[18] S. Acevedo, L. Giraldo, L. Giraldo, ACS Omega 5 (2020) 10423–10432, https://doi.org/10.1021/acsomega.0c00342.
[19] D.M. D'Alessandro, B. Smit, J.R. Long, Angew. Chem. Int. Ed. 49 (2010) 6058–6082, https://doi.org/10.1002/anie.201000431.
[20] A.A. Okesola, A.A. Oyedeji, A.F. Abdulhamid, J. Olowo, B.E. Ayodele, T.W. Alabi, IOP Conf. Ser: Mater. Sci. Eng. 413 (2018), 012077, https://doi.org/10.1088/1757-899x/413/1/012077.
[21] A. Mukherjee, J.A. Okolie, A. Abdelrasoul, C. Niu, A.K. Dalai, J. Environ. Sci. 83 (2019) 46–63, https://doi.org/10.1016/j.jes.2019.03.014.
[22] D.S. Ahmed, G.A. El-Hiti, E. Yousif, A.A. Ali, A.S. Hameed, J. Polym. Res. 25 (2018) 75, https://doi.org/10.1007/s10965-018-1474-x.
[23] T. Wilberforce, A. Olabi, E.T. Sayed, K. Elsaid, M.A. Abdelkareem, ci., Total. Environ. 761 (2021), 143203, https://doi.org/10.1016/j.scitotenv.2020.143203.
[24] O. Jankovský, M. Lojka, A.-M. Lauermannová, F. Antončík, M. Pavlíková, Z. Pavlík, D. Sedmidubský, Appl. Sci. 10 (2020) 2254, https://doi.org/10.3390/app10072254.
[25] K. Goh, H.E. Karahan, E. Yang, T.-H. Bae, Appl. Sci. 9 (2019) 2784, https://doi.org/10.3390/app9142784.
[26] A. Samanta, A. Zhao, G.K.H. Shimizu, P. Sarkar, R. Gupta, Ind. Eng. Chem. Res. 51 (2012) 1438–1463, https://doi.org/10.1021/ie200686q.
[27] J. Yen Lai, L.H. Ngu, S.S. Hashim, Greenh. Gases, Sci. Technol. 11 (2021) 1076–1117, https://doi.org/10.1002/ghg.2112.
[28] F. Raganati, F. Miccio, P. Ammendola, Energy Fuels 35 (2021) 12845–12868, https://doi.org/10.1021/acs.energyfuels.1c01618.
[29] V. Indira, K. Abhitha, I.O.P. Conf, Ser, Mater. Sci. Eng. 1114 (2021), 012081, https://doi.org/10.1088/1757-899X/1114/1/012081.
[30] Q. Wang, J. Luo, Z. Zhong, A. Borgna, Energ. Environ. Sci. 4 (2011) 42–55, https://doi.org/10.1039/C0EE00064G.
[31] Y. Shi, R. Ni, Y. Zhao, Energy Fuels 37 (2023) 6365–6381, https://doi.org/10.1021/acs.energyfuels.3c00381.
[32] S. Builes, P. López-Aranguren, J. Fraile, L.F. Vega, C. Domingo, Energy Fuels 29 (2015) 3855–3862, https://doi.org/10.1021/acs.energyfuels.5b00781.
[33] S. Wang, S. Yan, X. Ma, J. Gong, Energ. Environ. Sci. 4 (2011) 3805–3819, https://doi.org/10.1039/c1ee01116b.
[34] S.C. Lee, H.J. Chae, S.J. Lee, B.Y. Choi, C.K. Yi, J.B. Lee, C.K. Ryu, J.C. Kim, Environ. Sci. Tech. 42 (2008) 2736–2741, https://doi.org/10.1021/es702693c.
[35] J. Choma, M. Kloske, A. Dziura, K. Stachurska, M. Jaroniec, Eng. Prot. Environ. 19 (2016) 169–182. :10.17512/ios.2016.2.1.
[36] L. Hauchhum, P. Mahanta, J. Energy Environ. Eng. 5 (2014) 349–356, https://doi.org/10.1007/s40095-014-0131-3.
[37] Y.-C. Chiang, C.-Y. Yeh, C.-H. Weng, Appl. Sci. 9 (2019) 1977, https://doi.org/10.3390/app9101977.
[38] A.S. Aquino, M.O. Vieira, A.S.D. Ferreira, E.J. Cabrita, S. Einloft, M.O. De Souza, Appl. Sci. 9 (2019) 2614, https://doi.org/10.3390/app9132614.
[39] P. Staciwa, U. Narkiewicz, D. Sibera, D. Moszyński, R.J. Wróbel, R.D. Cormia, Appl. Sci. 9 (2019) 3349, https://doi.org/10.3390/app9163349.
[40] S. Choi, J.H. Drese, C.W. Jones, ChemSusChem 2 (2009) 796–854, https://doi.org/10.1002/cssc.200900036.
[41] R. Dawson, A.I. Cooper, D.J. Adams, Prog. Polym. Sci. 37 (2012) 530–563, https://doi.org/10.1016/j.progpolymsci.2011.09.002.
[42] W. Wang, M. Zhou, D. Yuan, J. Mater. Chem. A 5 (2017) 1334–1347, https://doi.org/10.1039/c6ta09234a.
[43] S.E.M. Elhenawy, M. Khraisheh, F. AlMomani, G. Walker, Catalysts 10 (2020) 1293, https://doi.org/10.3390/catal10111293.
[44] P. Kumar, B. Anand, Y.F. Tsang, K.-H. Kim, S. Khullar, B. Wang, Environ. Res. 176 (2019), 108488, https://doi.org/10.1016/j.envres.2019.05.019.
[45] O.G. Mousa, E. Yousif, A.A. Ahmed, G.A. El-Hiti, M.H. Alotaibi, D.S. Ahmed, Appl. Petrochem. Res. 10 (2020) 157–164, https://doi.org/10.1007/s13203-020-00255-7.
[46] A. Mohammed, E. Yousif, G.A. El-Hiti, Materials 13 (2020) 1183, https://doi.org/10.3390/ma13051183.
[47] Z.N. Mahmood, M. Alias, G.-A.-R. El-Hiti, D.S. Ahmed, E. Yousif, Korean J. Chem. Eng. 38 (2021) 179–186, https://doi.org/10.1007/s11814-020-0692-1.
[48] A.G. Hadi, K. Jawad, E. Yousif, G.A. El-Hiti, M.H. Alotaibi, D.S. Ahmed, Molecules 24 (2019) 1631, https://doi.org/10.3390/molecules24081631.
[49] H.A. Satar, A.A. Ahmed, E. Yousif, D.S. Ahmed, M.F. Alotibi, G.A. El-Hiti, Appl. Sci. 9 (2019) 4314, https://doi.org/10.3390/app9204314.
[50] E.D. Frohlich, Arch. Intern. Med. 140 (1980) 954–959, https://doi.org/10.1001/archinte.1980.00040020954016.
[51] M.J.K. Bichana, F.M. Abdoon, Asian J. Pharm. Clin. Res. 12 (2019) 366–371. 10.22159/ajpcr.2019.v12i3.30697.
[52] S.M. Ud Din, G. Mohan, T.P. Shukla, M. Ud Din, S. Sharma, I. Hassan, J. Glob, Trends,, Pharm. Sci. 5 (2014) 1912–1922.
[53] N.W. Alcock, J. Culver, S.M. Roe, J. Chem. Soc. Dalton Trans. 9 (1992) 1477–1484, https://doi.org/10.1039/DT9920001477.
[54] J. Barroso-Flores, R. Cea-Olivares, R.A. Toscano, J.A. Cogordan, J. Organomet. Chem. 689 (2004) 2096–2102, https://doi.org/10.1016/j.jorganchem.2004.03.035.
[55] M.S. Refat, N.M. El-Metwaly, Spectrochim. Acta A Mol. Biomol. Spectrosc. 81 (2011) 215–227, https://doi.org/10.1016/j.saa.2011.05.108.
[56] Y.A. Rasyda, S.B. Rahardjo, F. Nurdiyah, I.O.P. Conf, Ser, Mater. Sci. Eng. 578 (2019), 012008, https://doi.org/10.1088/1757-899X/578/1/012008.
[57] A.M. Donald, Nat. Mater. 2 (2003) 511–516, https://doi.org/10.1038/nmat898.
[58] K.W. Shinato, F. Huang, Y. Jin, Corros. Rev. 38 (2020) 423–432, https://doi.org/10.1515/corrrev-2019-0113.
[59] M. Thommes, K. Kaneko, A.V. Neimark, J.P. Olivier, F. Rodriguez-Reinoso, J. Rouquerol, K.S. Sing, Pure Appl. Chem. 87 (2015) 1051–1069, https://doi.org/10.1515/pac-2014-1117.
[60] O. Erdem, E. Yildiz, Inorg. Chim. Acta 438 (2015) 1–4, https://doi.org/10.1016/j.ica.2015.08.015.
[61] K.A. Cychosz, M. Thommes, Engineering 4 (2008) 559–566, https://doi.org/10.1016/j.eng.2018.06.00.
[62] M. Razavian, S. Fatemi, M. Masoudi-Nejad, Adsorpt. Sci. Technol. 32 (2014) 73–87, https://doi.org/10.1260/0263-6174.32.1.73.